

Disclaimer:

The contents of this report reflect the views of the authors, who are responsible for the facts and the accuracy of the information presented herein. This document is disseminated in the interest of information exchange. The report is funded, partially or entirely, under 69A3552348333 from the U.S. Department of Transportation's University Transportation Centers Program. The U.S. Government assumes no liability for the contents or use thereof.



**Transportation Infrastructure Precast Innovation Center
(TRANS-IPIC)**

University Transportation Center (UTC)

**Shape Memory Alloy Transverse Reinforcement for Precast Bridge
Girders End Regions**

Project No.: UI-23-RP-01

FINAL REPORT

Submitted by:

Principal Investigator: Professor Bassem Andrawes
University of Illinois at Urbana-Champaign
andrawes@illinois.edu

Ph.D. Student: Siyoung Park
University of Illinois at Urbana-Champaign

Collaborators / Partners:

- County Materials Corporation
- GTI General Technologies, Inc.

Submitted to:

TRANS-IPIC UTC
University of Illinois Urbana-Champaign
Urbana, IL

Executive Summary:

This project report evaluates the effect of SMA reinforcement as an end-region transverse reinforcement in precast concrete (PC) bridge girders using finite element (FE) analysis and experimental studies. In the FE analysis, a representative bridge girder model (Bulb Tee (BT)-72) was first numerically modeled and examined by evaluating the end region damage due to prestress release. Tensile damage index, crack area, and crack width were the parameters to assess the damages in end regions. Referring to the BT-72 model, stirrups in the end region were partially replaced with SMA stirrups. SMA stirrups' effectiveness was proven in reducing crack propagation by applying prestressing force vertically, improving the serviceability (durability) in the girder's end region.

Preliminary FE analysis was also performed to simulate the designed experimental specimens. Several models were tested to refer to designing girder models. After conducting experiments, models were modified to match the material properties, boundary conditions, and loading protocol and then analyzed to compare with the experiment results. By synchronizing the results, it was expected that diverse variables including dimensions, prestress value, and prestress location would be conveniently examined in future studies.

Precast prestressed concrete girders were prepared by testing the procedure for stretching prestressing strands in a fixed steel frame and wooden molds. The maximum prestress value was examined using the hydraulic jacking equipment available at the Newmark Structural Engineering Laboratory. The pump pressure to achieve a certain prestress level was experimentally studied.

Precast prestressed concrete girders with prestressing strands at the web and bottom flange were tested with steel stirrup-only and SMA stirrup-replaced models. Visual inspection and strain values were introduced to evaluate the SMA stirrup effect.

Finally, the effect of detailing the SMA stirrup was investigated, especially, the impact of heating the SMA on the the deformations experienced at the end hooks of the SMA bars. The movement effect of the SMA bar due to activation inside the concrete was experimentally investigated. By full activation, the longitudinal displacement of the SMA was measured and used to develop and calibrate a numerical model.

Table of Contents

Executive Summary	2
1. Project Description	4
1.1 Research plan – statement of problem	4
1.2 Research plan – summary of project activities	4
2. Project Progress	5
2.1 Finite element (FE) analysis on BT-72 precast prestressed girder	5
2.2 Case studies on reduced scale of AASHTO Type I girder	6
2.3 Experimental study on reduced AASHTO Type I girder	8
2.4 Comparison of experimental results and finite element FE analysis results	13
2.5 Experimental and numerical study on SMA opening effect	13
3. Educational Outreach Activities	15
4. Publications	15
5. Presentations and Posters	15
6. References	15

TRANS-IPIC Final Report:

1. Project Description

1. Research Plan - Statement of Problem

Despite the success of using concrete prestressing technology in the longitudinal direction, it has not been implemented in the transverse direction due to many practical challenges. The reason is that no practical method exists for prestressing internal shear reinforcement such as hoops, stirrups, or spirals because these reinforcements are fully embedded in the concrete; hence, gripping the reinforcement ends for prestressing is not feasible. This research investigated a new technology for applying prestressing in the transverse direction using a class of smart metallic materials known as shape memory alloys (SMAs). Excessively deformed bars and wires made of SMAs can remember their original shape when subjected to a temperature of approximately 200°C. This project utilized this novel material to solve the longstanding problem of splitting and bursting cracking at the end regions of precast concrete (PC) bridge girders. Applying prestressing in the transverse direction (i.e., vertically) within that local region will help mitigate concrete cracking during prestressing and reduce steel congestion in this region.

2. Research Plan - Summary of Project Activities

The behavior of the specimens was evaluated through a detailed finite element (FE) analysis. The end region behavior of the specimens at the web by prestressing strands was investigated using the amount of transverse steel specified by AASHTO. The effect of SMA reinforcement compared to the conventional (non-prestressed) reinforcement was also studied, focusing on the end region. The opening effect of the SMA bar during the activation was numerically modeled using the experimental data.

I-shaped precast prestressed girder specimens with conventional steel and SMA were fabricated and tested. Before casting, prestressing strands were tensioned, and then in the SMA specimen cases, SMA transverse reinforcement was placed at the specimen's ends and activated. Next, strands were detensioned, and vertical and horizontal strain progression at the end region was monitored.

The opening effect of the SMA hooked ends was experimented solely and within the concrete. The straight and curved parts of the SMA were pre-strained and heated beyond 200°C. During the experiments, the opening displacement of the SMA hooks was measured and crack/damage progression in concrete was visually inspected. After conducting experiments, numerical modeling was conducted based on the results.

2. Project Progress

1. Finite element (FE) analysis on BT-72 precast prestressed girder

The finite element (FE) method was employed to examine numerically the feasibility of the new concept of applying transverse prestressing to mitigate the end region damages due to the transfer of prestressing force. The concept of the study was first examined by evaluating the end region damage of the BT-72 girder caused by prestress transfer using the FE program ABAQUS. The girder model had a length of 121 ft with a designed concrete strength of 6.5 ksi. The low-relaxation seven-wire strand with a diameter of 0.5 in. and ultimate strength of 270 ksi was placed straight at the bottom flange and in a harped shape at the top flange of end regions. The strand numbers at each location were thirty-six and twelve at the bottom and top of the girder. The double-legged #5 steel stirrups were placed at 4 in. spacing and #4 confinement reinforcements at 6 in. spacing at the end region (**Figure 1**).

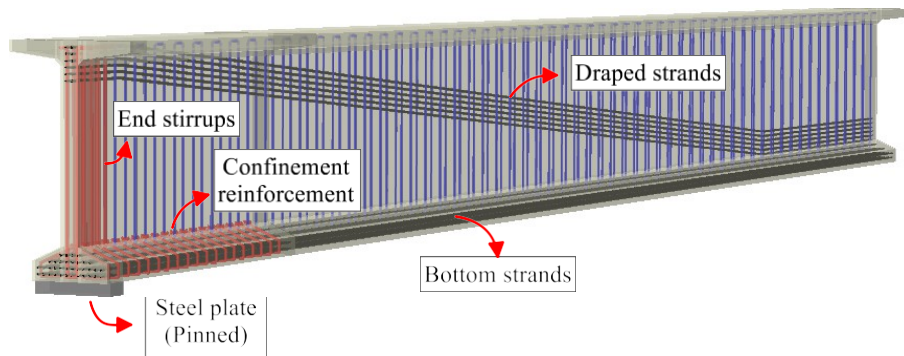
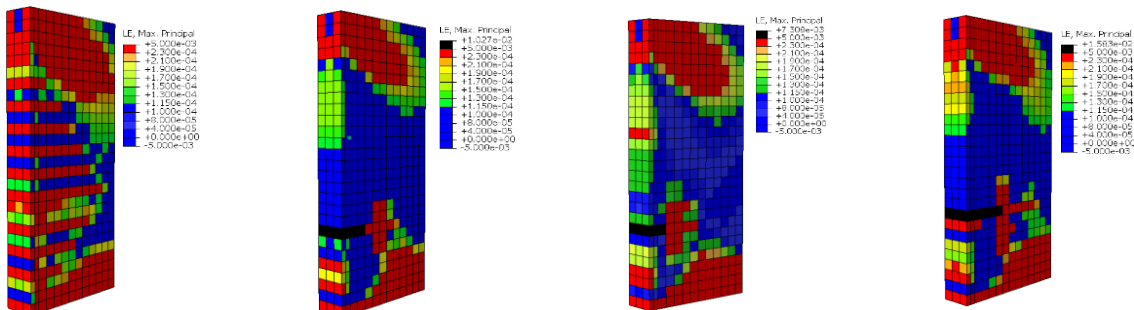


Figure 1. Finite element model of the BT-72 girder considered in the analysis

In the numerical analysis, four cases were compared in terms of cracked area and crack width to assess the extent of end damage. The steel case is labeled BT-72, whereas girders with SMA stirrups are labeled 5S2, 5S1, and 3S1. The naming was decided based on the number of end stirrups (3 and 5) and the number of SMA stirrups at the end region (1 and 2). **Figures 2(a) – (d)** visually show the cracked area in the web region. As SMA stirrups were added in the end region of a girder, prestressing force reduced a significant amount of splitting crack propagation.

A single SMA was also effective, representing better performance with fewer end stirrups (case (d)). **Figure 2(e)** shows the exact amount of crack reduction, in which one or two SMA stirrups at the end region reduced the crack area of the web by up to 53% and crack width by distance from the end face in each model. Crack widths in SMA models were below 0.007 in. at the surface of the web, proving SMA stirrups' capability of improving serviceability (durability) in the end region of girders.



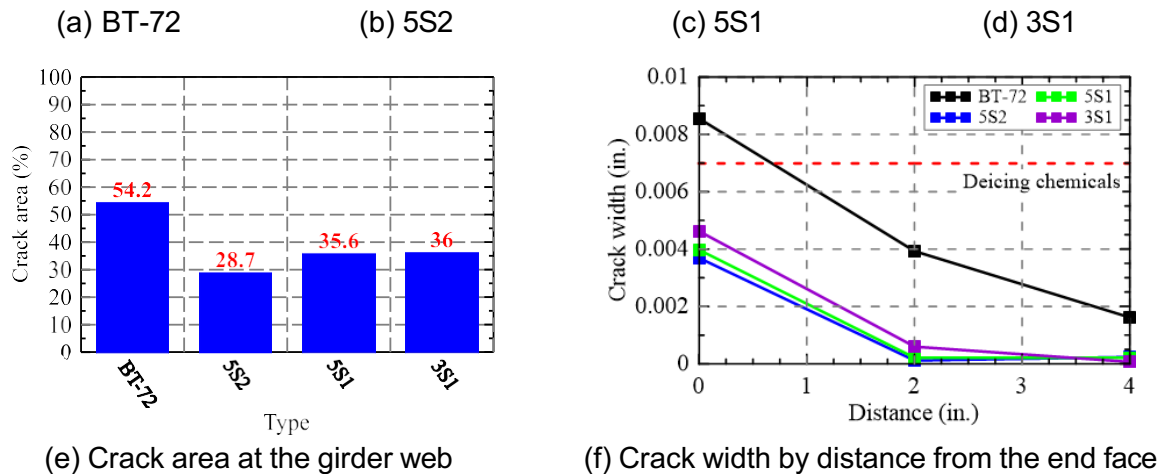


Figure 2. Numerical analysis results

2. Case studies on reduced scale of AASHTO Type I girder

After performing FE analysis on the BT-72 girder, the next step was to examine damages in a reduced girder scale, which progressed as a preliminary analysis for the experimental study. The AASHTO Type I girder was set as a control model and the size of the girder model was reduced to half its original size. Parametric studies on the number and location of the prestressing strand in the girder were conducted to decide which model would detect the crack/damage on the non-prestressed reinforcement model. In contrast, the SMA reinforcement model was evaluated to validate the effect of the transverse SMA reinforcement model.

Figure 3 shows five cases that were evaluated through the FE analysis. In the prestressing test setup, the prestressing force of 24 kips was measured to be the maximum value that could be achieved. Thus, each strand was designed to have 24 kips of detensioning forces. After all, case 1 was chosen to be tested experimentally to understand the prestress release effect in terms of horizontal and vertical strain/stress and end damage.

The case 1 design was numerically modeled with the conventional steel stirrup and SMA stirrup to compare the horizontal and vertical strain development as per the prestressing force increases. **Figure 4** shows the strain history at four different locations, R1, R2, R3, and R4. The locations are at the concrete surface parallel to the prestressing strand, at a distance of 0.875, 1.75, 2.625, and 3.5 in., which are under the end region of the girder. By using the SMA stirrup, the vertical strain value was significantly dropped, proving the effectiveness of the new concept.

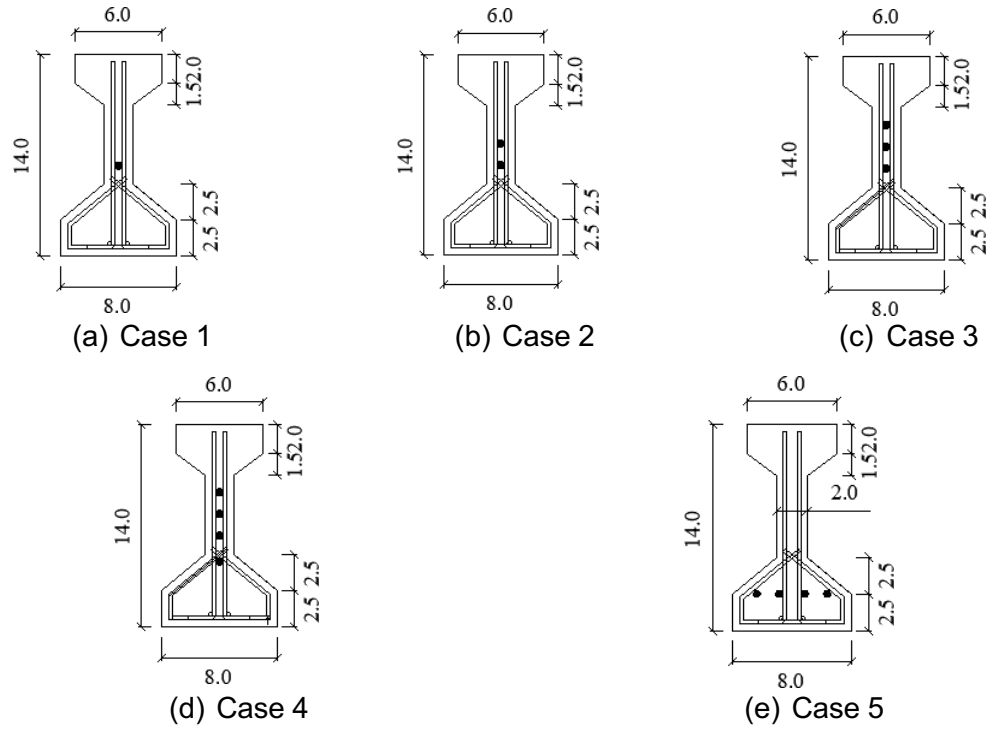


Figure 3. Prestressing strand layouts

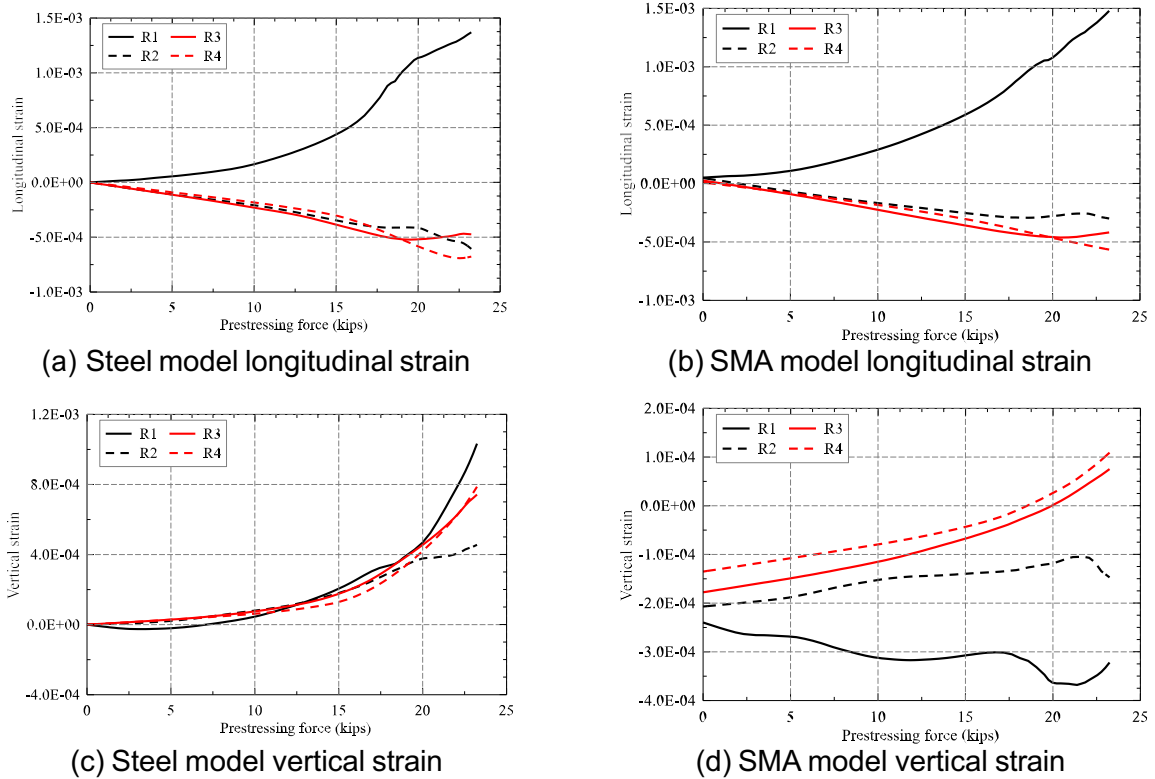


Figure 4. Strain history at the concrete surface by detensioning

A shear loading analysis was also performed using a displacement control method with a load plate at a distance of $h/2$ (7 in.) from the end face. The displacement gradually increased to 0.2 in., and tensile damage was evaluated to compare the steel and SMA reinforcement models. **Figure 5** shows the damage pattern at 0.1 and 0.2 in. displacements. A single transverse SMA showed that the prestressing force of the SMA stirrup resisted the shear cracks effectively at 0.1 in. displacement. The shear failure mechanism was transitioned to the flexural cracking mechanism by applying SMA prestressing force.

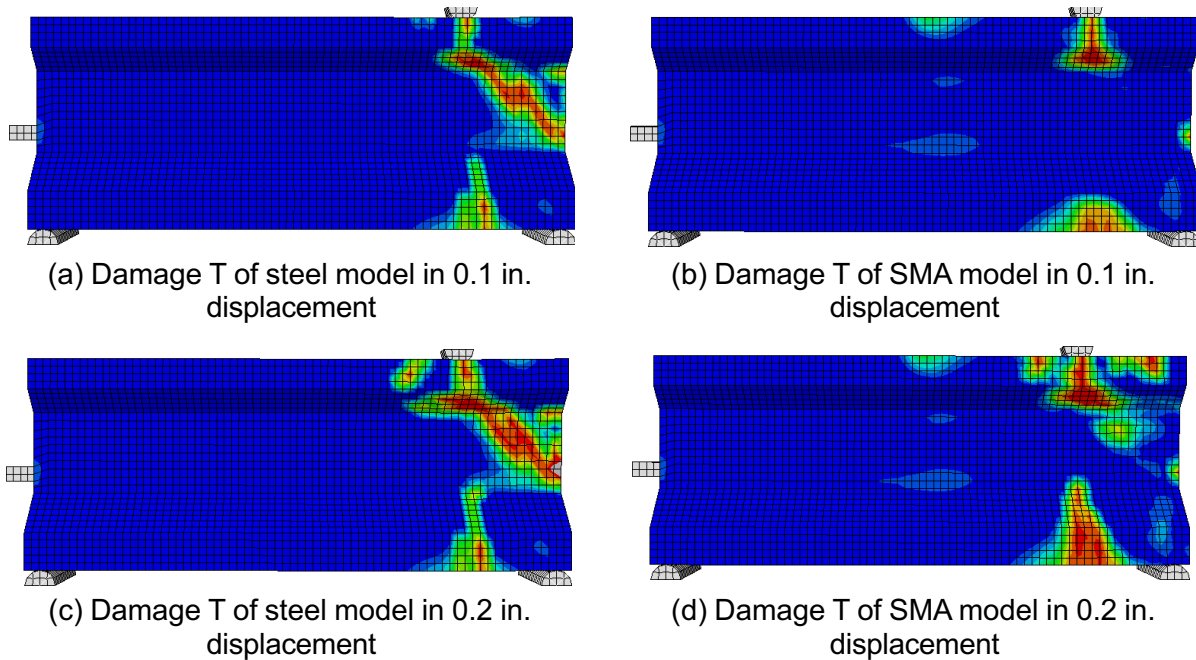


Figure 5. Damage progression by shear loading

3. Experimental study on reduced AASHTO Type I girders

The experimental specimens designed based on the FE analysis were tested in the following sequence. First, the maximum force that prestress release can achieve was confirmed by stretching it with a pump in a fixed steel frame, and then de-tensioning using the flame torch (Figure 6).



Figure 6. Pre-tensioning process of a prestressing strand

The strands' prestressing force was measured through a load cell by changing the pump pressure from 2000 to 5200 psi. At 2000 psi pump pressure, the measured prestressing force was 11.5 kips; at 5200 psi pump pressure, the prestressing force was 31.4 kips. After detaching the pump, the final prestressing force prestress losses due to elastic shortening and anchorage setting was measured as 24 kips, which is 25% less than the initial prestressing force. For future experiments, the prestressing force of 24 kips was assigned in designing experimental plans.

Referring to the numerical analysis results, the specimen dimensions were designed as shown in **Figure 7**. The stirrups were located at a spacing of 6 in. with a size of #2 ($d = 0.25$ in.) to match the size of the NiTiNb bar ($d = 0.236$ in.). The confinement reinforcement also had a diameter of 0.25 in. (#2) and was placed in a spacing of 6 in. The specimen length was designed to be 3 ft due to the length limitation of the steel frame (pre-straining test bed setup). The self-consolidated concrete has been planned to be used in casting concrete since vibrating the concrete was unavailable during casting. The mixture design was set by ACI 237R-07.

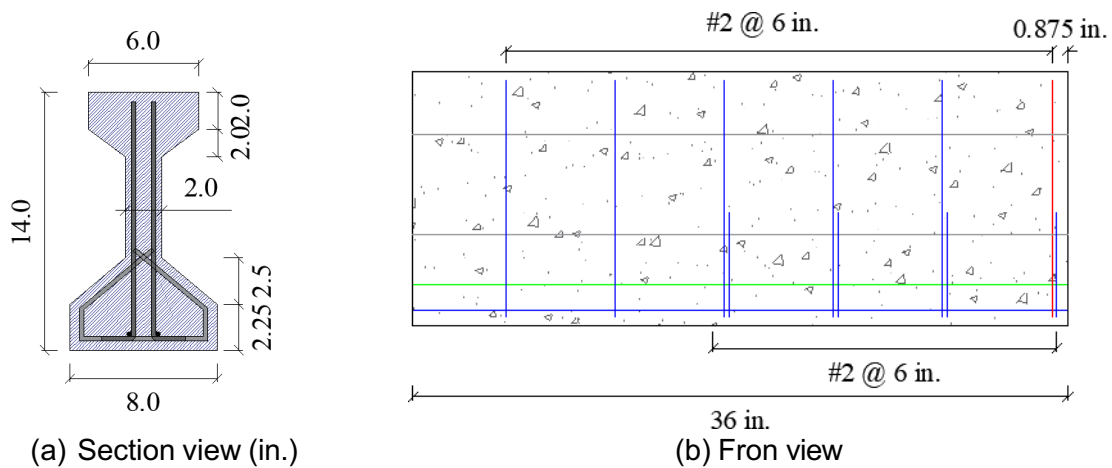


Figure 7. Specimen dimensions

Figure 8 shows the procedure for manufacturing specimens. The I-shaped girder was made by attaching two side faces on the bottom plate. Stirrups were fixed in position relying on the longitudinal bar and prestressing strand. Wood spacers were anchored to the steel stirrup to secure the stirrups' spacing. After demolding wood molds, concrete strain gages were attached at the end face of web regions in horizontal and vertical directions.



(a) Steel stirrup specimen



(b) SMA stirrup specimen



(c) Concrete casting



(d) Completed specimens

Figure 8. Specimen fabricating procedure

In the SMA reinforcement specimen, SMA activation testing was first conducted. As shown in **Figure 9**, vertical strain at the concrete surface was measured, which was located at 0.875, 1.75, and 2.625 in. from the end face. At the first activation, compressive strain with a maximum value of $25 \mu\epsilon$ was applied 0.875 in. from the end, which matches well with the theoretical calculations. After the second activation, the compressive stress of $121 \mu\epsilon$, $75 \mu\epsilon$, and $35 \mu\epsilon$ was developed at strain gages located at 0.875, 1.75, and 2.625 in., respectively from the end of the specimen. Throughout the experiment, it was proven that SMA prestressing force was sufficiently transferred to the concrete. Also, the prestressing force by SMA activation was linearly transferred throughout the concrete surface, being maximum near the end face.

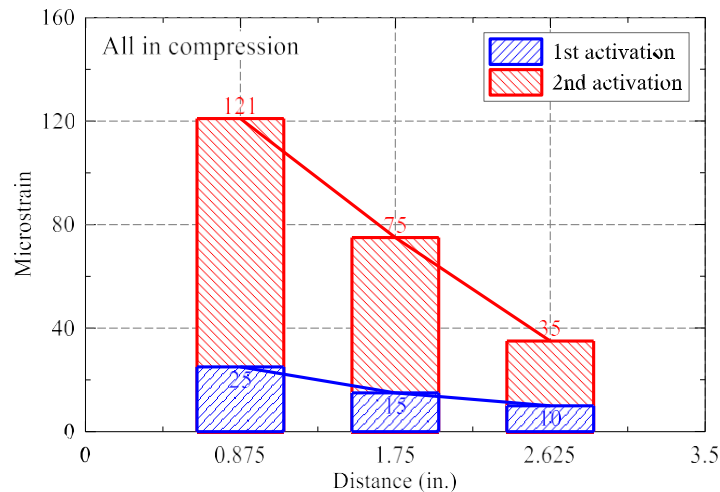


Figure 9. Compressive stress on concrete during activation

After activating the SMA stirrups, prestress release testing was conducted on steel and SMA specimens. “H1” and “H2” are concrete strain gages installed at 1.75 in. and 7.75 in. from the end face, parallel to the prestressing strand. “S1L1”, “S1R1”, “SMAL1”, and “SMAR1” are steel strain gages installed at the end stirrup next to the prestressing strand. **Figure 10** shows the test results. The compressive strain was well developed along the prestressing strands in the steel reinforcement specimen, experiencing a compressive microstrain of $80 \mu\epsilon$ at H2. Comparing the vertical strain at the V2 where stirrups were located, the steel reinforcement specimen reached a maximum tensile strain of $50 \mu\epsilon$. In contrast, the SMA reinforcement specimen started from

compressive strain, reaching $25 \mu\epsilon$ without experiencing any sudden increase in tensile strain. The compressive force generated by SMA activation was proven effective in preventing unexpected tensile strains but stabilizing their growth.

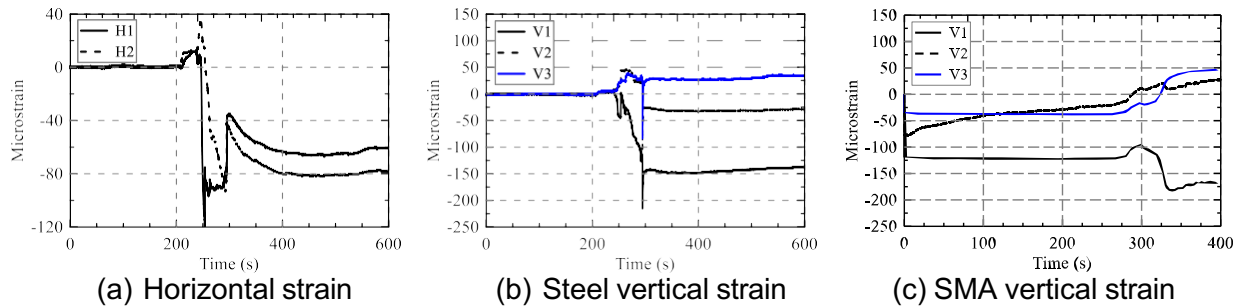


Figure 10. Strain development by prestress release

In the experiment with a single prestressing strand, the tensile damage was mainly due to the axial load in releasing the prestress. A new experiment was designed to induce tensile strain by moment force by placing prestressing strands at the bottom flange. **Figure 11** shows the section view of the new specimen. Four prestressing strands were located at a height of 1.5 in. The outer prestressing strands were designed to release first and then the inner strands. Single-legged stirrups were used in the new specimen to enhance the probability of propagating cracks.

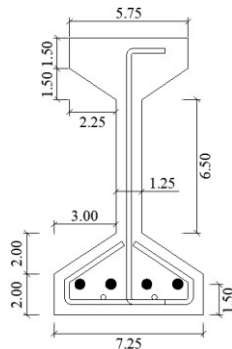


Figure 11. Section view of specimen with four prestressing strands

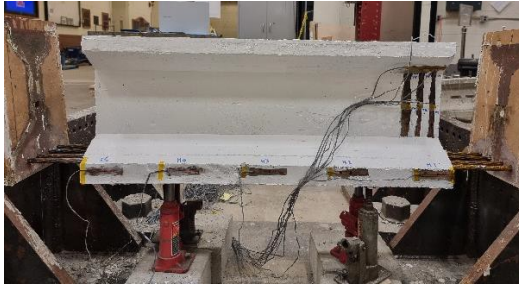
Figure 12 shows the fabrication procedure of the specimen. The steel cage was first assembled and then put into the wood mold. After casting self-consolidated concrete, it was painted in white color to detect cracks more easily. Five horizontal strain gages (H1 to H5) were attached parallel to the prestressing strand and six vertical strain gages (V1b, V1t, V2b, V2t, V3b, and V3t) were installed at the web region of the end face. “V1”, “V2”, V3” stands for the distance from the end face, which is 0.75, 2.0, and 3.25 in., respectively. “b” stands for the bottom, and “t” stands for the top.



(a) Steel frame



(b) Steel and wood mold assembly



(c) Specimen preparation

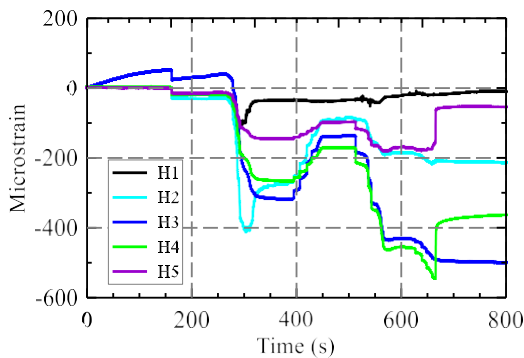


(d) Strand cut

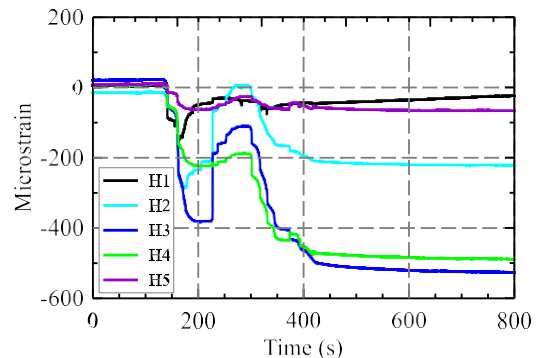
Figure 12. Specimen fabricating procedure

Figure 13 shows the strain development at each cutting phase. As shown in **Figures 13(a)** and **(b)**, the compressive strain at both ends was almost zero, increasing to a maximum in the middle of the specimen. The maximum compressive strain/stress was $500 \mu\epsilon$ (2.5 ksi).

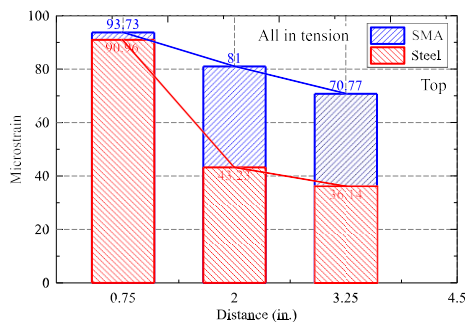
Figures 13 (c) and **(d)** show the maximum vertical strain at the top and bottom of the end face during de-tensioning prestress by distance from the end face. All locations were below the cracking strain of $130 \mu\epsilon$, showing no visual cracking. The most crack-vulnerable region is at a distance of 0.75 in. from the end face. As shown in **Figure 13 (d)**, the vertical SMA reinforcement affects the bottom of the web, dropping $5.5 \mu\epsilon$. Although the effectiveness was not significant, it should be noted that only a single SMA was used, which has almost $\frac{1}{4}$ of the elastic modulus compared to conventional reinforcing bars.



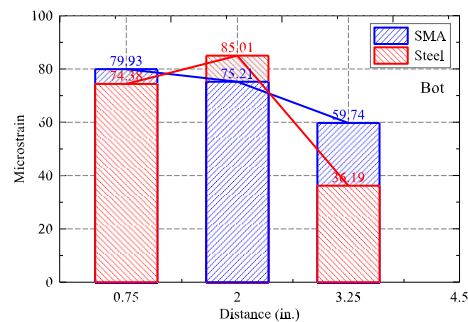
(a) Horizontal strain in steel specimen



(b) Horizontal strain in SMA specimen



(c) Vertical strain at the top of the web

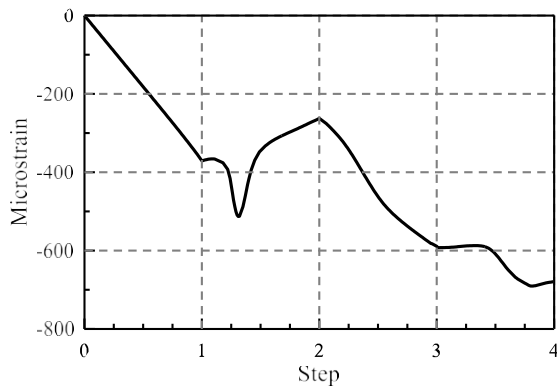


(d) Vertical strain at the bottom of the web

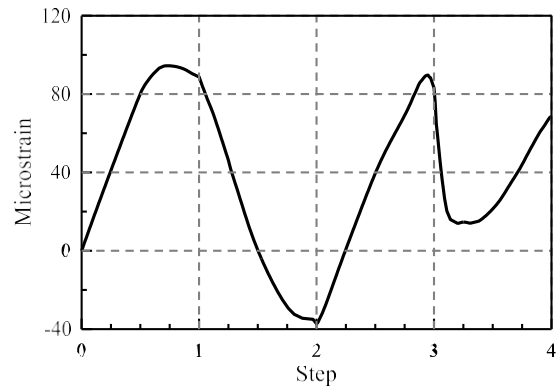
Figure 13. Experiment results during prestress release at the concrete surface

4. Comparison of experimental results and finite element FE analysis results

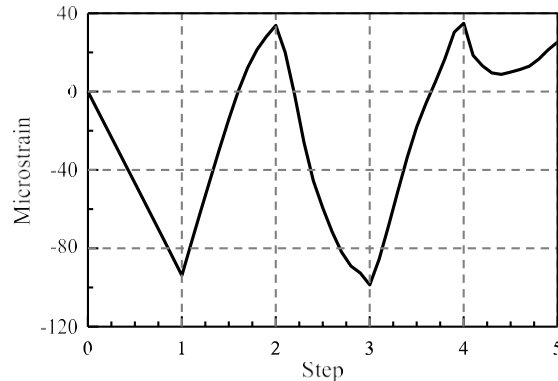
The numerical analysis reviewed the final stage of the steel specimen experiment. Strain distribution and horizontal and vertical strains were compared by replicating the experimental model. These results anticipate the tensile strain progression in SMA reinforcement specimens. **Figure 14** shows the numerical analysis results. **Figure 14(a)** is the strain variation at the center of the concrete surface in the bottom flange, which is parallel to the prestressing strand (H3). The microstrain was developed in compression in the sequence of $-500 \mu\epsilon$, $-280 \mu\epsilon$, $-600 \mu\epsilon$, and $-700 \mu\epsilon$, with a trend that matched well with the experimental results (**Figure 13(a)**). **Figure 14(b)** shows the vertical strain variation at the bottom of the web, 0.75 in. from the end face. The results also resembled the experimental result (**Figure 14(b)**), showing a maximum tensile microstrain of $95 \mu\epsilon$. The tensile strain developed when strands near the side face were released, whereas compressive strain formulated when opposite side strands were released. Moving on to the SMA reinforcement model (**Figure 14(c)**), due to the presence of vertical prestressing force (step 1), the maximum tensile strain was reduced to $30 \mu\epsilon$, indicating the effectiveness of vertical SMA reinforcement.



(a) Horizontal strain at H3 location in the steel reinforcement girder model



(b) Vertical strain at the V1b location in the steel reinforcement model



(c) Vertical strain at the V1b location in the SMA reinforcement model

Figure 14. Numerical analysis results

5. Experimental and numerical study on SMA end hook opening effect

A study was carried out to investigate the impact of heating the SMA on the deformations occurring at the hooked end of the embedded SMA bar. The SMA bent at 90 degrees was thermally triggered using an induction coil. **Figure 15** shows the test setup. The heating area was

concentrated at the bent regions to solely evaluate the opening occurring at the bent region. Two pre-strained and without pre-straining specimens were heated beyond 200°C to activate the SMA fully. A specimen without pre-straining showed 0.2 in. displacement in the longitudinal direction, whereas a pre-strained specimen experienced 0.65 in. displacement.

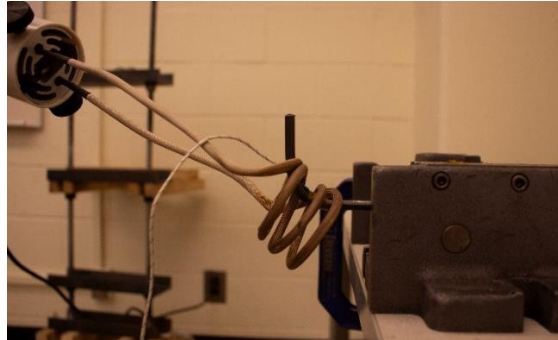


Figure 15. Induction heating performed on 90 degrees hooked SMA bar

Next, the opening effect of the SMA hook inside the concrete was evaluated with three different specimens. **Figure 16** shows the experimental and numerical analysis results. The clear cover (0.5 in. and 1.0 in.) and pre-straining were two variables controlled. “PB” is the specimen prestrained, “B” is the specimen without prestraining, “1” is for clear cover of 1.0 in., and “05” is for clear cover of 0.5 in. The concrete height was designed to be equal to the SMA bar. Digital image correlation (DIC) was used to track strain development. The clear cover was the dominant factor to prevent crack propagation and the presence of prestraining also increased cracks in bent regions.

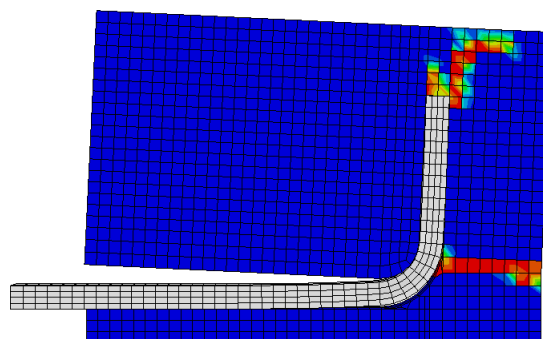
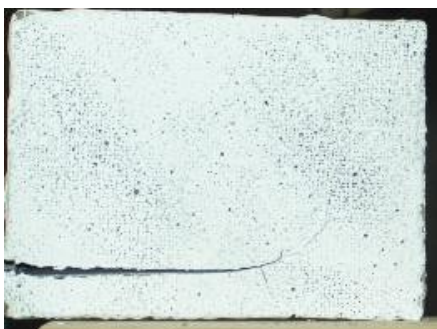
Numerical modeling was performed using the experimental results with induction heating of the bent SMA. In numerical modeling, thermal expansion was controlled in four segmented sections to imitate the opening effect. As shown in **Figure 16(d)** the numerical analysis matched well with the experimental results.



(a) B-1 specimen



(b) B-05 specimen



(c) PB-1 specimen

(d) Numerical analysis result of B-05

Figure 16. SMA opening effect on concrete after SMA activation

3. Educational Outreach Activities

- Park, S., and Andrawes, B. "Shape Memory Alloy Transverse Reinforcement for Solving End Region Problems in Precast Bridge Girders", *TRANS-IPIC Monthly Research Webinar*, 02/19/2024.
- Park, S., and Andrawes, B. "PC Girders End Region Damage Mitigation Using Shape Memory Alloys", *2024 TRANS-IPIC UTC Workshop*, 04/22/2024.

4. Publications

- Park, S., and Andrawes, B. "Application of NiTiNb Shape Memory Alloys in the End Region of Prestressed Girders", *Advances in Structural Engineering*. (Submitted)

5. Presentations and Posters

- Park, S. and Andrawes, B. "Damage Mitigation of Prestressed Girders End Regions Using Shape Memory Alloys" *2024 Transportation Research Board Annual Meeting*
- Park, S. and Andrawes, B. "Transverse Prestressing of Prestressing of End Regions of Pretensioned Concrete Bridge Girders" *2025 Structures Congress*, Apr. 2025. (Accepted)

6. References

- *ACI Committee 237. (2007). Self-Consolidating Concrete, American Concrete Institute, Farmington Hills, MI, USA.*
- *American Association of State Highway and Transportation Officials. (2012). AASHTO LRFD Bridge Design Specifications, 6th ed., Washington DC, USA.*
- *PCI (Precast/Prestressed Concrete Institute). (2014). PCI Bridge Design Manual. 3rd ed. Second Release, Chicago, IL, USA.*